

Out of plane screening and dipolar interactions in heterostructures

Cheung Chan and T. K. Ng

Department of Physics, Hong Kong University of Science and Technology, Clear Water Bay, Kowloon, Hong Kong, China

(Dated: November 19, 2021)

Out-of-plane screening (OPS) is expected to occur generally in metal-semiconductor interfaces but this aspect has been overlooked in previous studies. In this paper we study the effect of OPS in electron-hole bilayer (EHBL) systems. The validity of the dipolar interaction induced by OPS is justified with a RPA calculation. Effect of OPS in electron-hole liquid with close-by screening layers is studied. We find that OPS affects the electronic properties in low density and long wavelength regime. The corresponding zero-temperature phase diagram is obtained within a mean field treatment. We argue that our result is in general relevant to other heterostructures. The case of strongly correlated EHBL is also discussed.

PACS numbers: 77.80.bn, 71.35.Ee, 71.35.-y

I. INTRODUCTION

Modern micro-electronics relies to a large degree on surface science, which concerns the material properties near a surface or interface. To enhance the performance of such devices, knowledge of the electronic states near the interfaces is required. Near a surface or interface, electronic reconstruction may alter three key factors - interaction strengths, bandwidths and electron densities [1] which determine electronic states and their properties.

In this paper, we consider another factor - the modification in form of interaction between electrons. For instance, in an insulator-semiconductor-insulator superstructure, if the dielectric constant of the semiconductor is sizably larger than that of insulator (barrier layer), the image charges induced at semiconductor-insulator interface can substantially enhance the binding energy of the excitons confined in the semiconductor layer [2, 3]. In this case, the electrons and holes do not interact via usual Coulomb potential after the effect of the image charges at the semiconductor-insulator interface is taken into account.

Recently, Huang *et al.* observed non-activated electronic conductivity of a two-dimensional (2D) low density hole system in a heterojunction insulated-gate field-effect transistor [4]. Such non-activated conductivity is unexpected as at low charge density strong Coulomb interaction is expected to crystallize the system (Wigner crystal), which is then pinned by disorder resulting in insulating behavior and activated conductivity. Huang *et al.* attribute the behavior to the screening of Coulomb interactions by the metallic gate, which leads to destruction of the Wigner crystal phase. Physically, the metallic gate which is located at a distance away from the 2D hole gas, provides an out of plane screening (OPS) to the hole-hole interaction, resulting in effective dipolar interaction between holes. Microscopically, when a charge is placed near a metal surface, an image charge of opposite sign will be induced at the surface to screen out the (static) electric field from the charge. From elementary electrostatics, the system can be described equivalently as a dipole formed by the charge and its image charge and the in-

teraction between two charges located near the interface changes from a Coulomb potential $\sim 1/r$ to a dipolar potential $\sim 1/r^3$. This modified interaction, which is generally expected to exist in metal-semiconductor heterostructures, can change the electronic properties near the interface. Unexpectedly, there has been no detailed theoretical study of this effect on electronic properties until recently [5]. The neglect of OPS might be due to dynamical screening of in-plane charges [5]. For high charge density, the screening can effectively reduce both Coulomb and dipolar interactions to short range interactions. However for low charge density electronic liquids in-plane screening is less effective and OPS can lead to a difference, as is observed by Huang *et al.* [4].

In this paper, we study how OPS affects the electronic properties in systems with two-layer of charges of opposite sign, i.e. the 2D electron-hole bilayer (EHBL) system. We shall study how OPS affects Wigner crystallization and exciton condensate in the system [4, 6] and will also comment on the effect of OPS in interfaces between metals and strongly correlated electron systems [7–9].

II. OPS AND EFFECTIVE INTERACTION BETWEEN CHARGES

In this section we provide the details for the EHBL systems we study and the corresponding OPS effective interaction. We shall assume that the only effect of the metallic screening layers is to provide an image charge for point charges sitting close to it and the effective interaction between charges will be derived from the image charge picture. The validity of this approximation is bounded by the plasma frequency $\omega_p^{(s)}$ of the screening layer, above which the screening layer cannot respond rapidly to the charge fluctuations. Thus our approximation is valid when the plasma frequency of the EHBL layer ω_p is much less than $\omega_p^{(s)}$, or that the screening layer has density of electric charge much larger than the charge density of the EHBL layers we consider. The image charge picture can be justified by a Random Phase Approximation (RPA) calculation which is shown in the

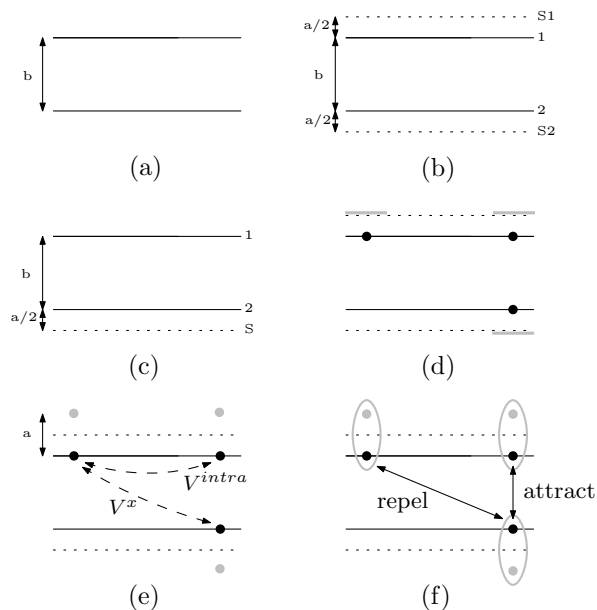


FIG. 1: (a) EHL system separated by distance b . (b) EHL with OPS by metallic plates in both layers. Dotted line represents metallic interface, separated from the main layer by a distance of $a/2$. (c) Similar to (b) but with only one OPS layer. (d) Charges (black dots) and screening charge response at the metal interface (grey patches). (e) Effective image charge (grey dots) and effective interactions V^{intra} and V^x . (f) Charges attract when they are aligned while they are not. This behavior is different from the Coulomb potential which is always attractive for a pair of electron and hole. The repulsive behavior inhibits exciton pairing.

Appendix.

Starting with a EHL system (Fig. 1(a)), two metallic screening layers can be added as shown in Fig. 1(b), or a single metallic screening layer can be added as shown in Fig. 1(c). We first consider the two-layer case (b). Fig. 1(d) depicts the charge response in the metallic layer to a nearby charge. The charge response is assumed to be an image charge, which carries opposite charge of the same magnitude and is centered at distance a from the point charge. Thus the point charge and the screening charge together form a dipole. We have assumed that the distance between the two layers of charges b is sufficiently larger than a ($b \gg a$) such that the presence of the other screening layer does not affect the simple dipole picture. In this case, the intralayer interaction between two charges located in an OPS layer (Fig. 1(e)) is in real space

$$V^{\text{intra}}(\vec{r}) = \frac{e^2}{\epsilon_{e,h}} \left(\frac{1}{r} - \frac{1}{\sqrt{r^2 + a^2}} \right), \quad (1)$$

where r is the charge-charge distance within the charge plane.

It is easy to see that for $r \gg a$, V^{intra} scales as $1/r^3$ while for $r \ll a$ it follows the usual Coulomb scaling $1/r$. By using 2D Fourier transform $\frac{1}{\sqrt{r^2 + a^2}} \xrightarrow{2D\mathcal{F}} \frac{2\pi}{k} e^{-ka}$, the

Fourier transformed interaction is

$$V^{\text{intra}}(\vec{k}) = \frac{2\pi e^2}{\epsilon_{e,h} k} (1 - e^{-ka}). \quad (2)$$

For an electron and a hole sitting in different layers, the interlayer interaction is

$$V^{x,2}(\vec{r}) = -\frac{e^2}{\epsilon_x} \left(\frac{1}{\sqrt{r^2 + b^2}} - \frac{2}{\sqrt{r^2 + (a+b)^2}} + \frac{1}{\sqrt{r^2 + (2a+b)^2}} \right)$$

and its Fourier counterpart is

$$V^{x,2}(\vec{k}) = -\frac{2\pi e^2}{\epsilon_x k} e^{-kb} (1 - e^{-ka})^2. \quad (3)$$

$\epsilon_{e,h}$ and ϵ_x are the intra-layer and inter-layer dielectric constants, respectively.

Next we consider EHL with only one metallic screening layer (see Fig. 1(c)). In this case the two layers of charges have distance $a/2 + b$ (layer 1) and $a/2$ (layer 2) from the screening layer, respectively. The intralayer interactions are thus

$$V_1^{\text{intra}}(\vec{r}) = \frac{e^2}{\epsilon_1} \left(\frac{1}{r} - \frac{1}{\sqrt{r^2 + (a+2b)^2}} \right),$$

$$V_2^{\text{intra}}(\vec{r}) = \frac{e^2}{\epsilon_2} \left(\frac{1}{r} - \frac{1}{\sqrt{r^2 + a^2}} \right).$$

with corresponding Fourier transforms

$$V_1^{\text{intra}}(\vec{k}) = \frac{2\pi e^2}{\epsilon_1 k} (1 - e^{-k(2b+a)}), \quad (4)$$

$$V_2^{\text{intra}}(\vec{k}) = \frac{2\pi e^2}{\epsilon_2 k} (1 - e^{-ka}).$$

The corresponding intralayer interaction is given by

$$V^{x,1}(\vec{r}) = -\frac{e^2}{\epsilon_x} \left(\frac{1}{\sqrt{r^2 + b^2}} - \frac{1}{\sqrt{r^2 + (a+b)^2}} \right)$$

and

$$V^{x,1}(\vec{k}) = -\frac{2\pi e^2}{\epsilon_x k} e^{-kb} (1 - e^{-ka}). \quad (5)$$

III. COLLECTIVE DENSITY RESPONSES

In this section we study the collective density responses of the EHL systems we considered. For a two component electronic system, the density-density response of the system is described by a 2×2 matrix $\chi_{ij}(q, \omega)$ with $i, j = 1, 2$. The density-density response matrix is given in RPA by [10]

$$\begin{pmatrix} \chi_{11} & \chi_{12} \\ \chi_{21} & \chi_{22} \end{pmatrix} = \frac{1}{\kappa} \begin{pmatrix} (1 - \chi_{02}V_{22})\chi_{01} & \chi_{01}V_{12}\chi_{02} \\ \chi_{02}V_{21}\chi_{01} & (1 - \chi_{01}V_{11})\chi_{02} \end{pmatrix} \quad (6)$$

where

$$\kappa(q, \omega) = (1 - \chi_{01}(q, \omega)V_{11}(q))(1 - \chi_{02}(q, \omega)V_{22}(q)) - \chi_{01}(q, \omega)V_{12}(q)\chi_{02}(q, \omega)V_{21}(q), \quad (7)$$

$V_{ij}(q)$ is the “bare” interaction between i^{th} and j^{th} components of the electronic liquid and

$$\chi_{0i}(q, \omega) = g_s \int \frac{d^2k}{(2\pi)^2} \frac{n_F(\varepsilon_k^{(i)}) - n_F(\varepsilon_{k+q}^{(i)})}{\hbar\omega + \varepsilon_k^{(i)} - \varepsilon_{k+q}^{(i)}}, \quad (8)$$

where $\varepsilon_k^{(i)} \sim k^2/2m^{(i)}$ is kinetic energy of species i particles (of mass $m^{(i)}$), n_F is the Fermi-Dirac distribution function and $g_s = 2$ is spin degeneracy. In the case of two screening layers the interactions $V_{11(22)}$ and $V_{12} = V_{21}$ are given by $V^{\text{intra}}(q)$ (eq. (2)) and $V^{x,2}(q)$ (eq. (3)), respectively whereas they are given by $V_{1(2)}^{\text{intra}}(q)$ (eq. (4)) and $V^{x,1}(q)$ (eq. (5)), respectively if there is only one screening layer.

Next we study the collective excitations (i.e. plasmons) in the system. The dispersion of the collective excitations are given by the equation

$$\kappa(q, \omega(q)) = 0. \quad (9)$$

We shall first consider the long wavelength limit ($q \rightarrow 0$) where the equation can be studied analytically. In this limit it is easy to show that

$$\chi_0(q, \omega) = \frac{n}{m} \left(\frac{q}{\omega}\right)^2 + \mathcal{O}\left(\left(\frac{q}{\omega}\right)^4\right), \quad (10)$$

where $n = \frac{g_s(\pi k_F^2)}{(2\pi)^2}$ is carrier density. We have neglected the component index i for brevity.

We begin with the Coulomb case (no screening layer). The interactions are respectively $V_{1,2}(q) = \frac{2\pi e^2}{\epsilon_{1,2}q}$ and $V_x(q) = -\frac{2\pi e^2}{\epsilon_x q} e^{-qb} \sim -\frac{2\pi e^2}{\epsilon_x q}$ for $q \ll b^{-1}$. The plasmon equation in $q \rightarrow 0$ limit reads

$$1 - 2\pi e^2 \left(\frac{n_1}{m_1 \epsilon_1} + \frac{n_2}{m_2 \epsilon_2} \right) \frac{q}{\omega^2} + (2\pi e^2)^2 \times \frac{n_1 n_2}{m_1 m_2} \left[\frac{1}{\epsilon_1 \epsilon_2} - \frac{1}{\epsilon_x^2} \right] \left(\frac{q}{\omega^2} \right)^2 = 0. \quad (11)$$

We first consider the case $\epsilon_x^2 = \epsilon_1 \epsilon_2$ such that the term in the square bracket is zero. In this case we need to expand the interlayer interaction to one order higher in q . As a result the last term in eq. (11) is replaced by a term of order $\frac{q^3}{\omega^4}$ and the plasmon equation at long wavelength limit yields two solutions, which are the out-of-phase mode ($\omega \sim q$) and in-phase mode ($\omega \sim \sqrt{q}$). Indeed this occurs usually in a 2D electronic systems with

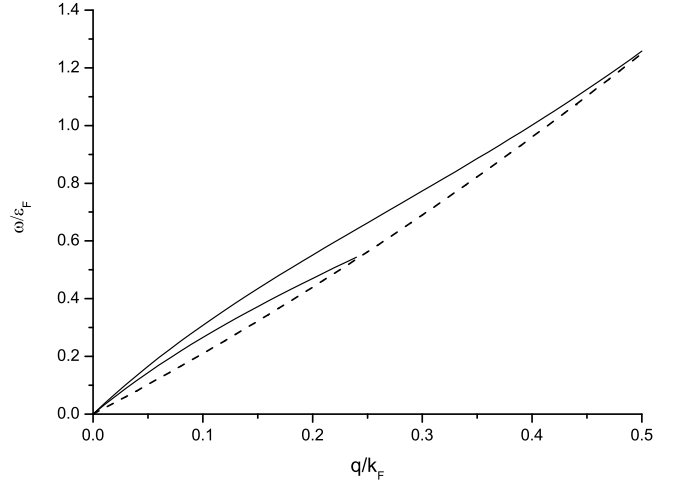


FIG. 2: Plasmon excitations in EHL with two screening layers computed numerically. The spectrum is computed by solving eq. (9) numerically with the full expression of $\chi_0(q, \omega)$ [10]. The solid lines are the plasmons excitations and the dash line represents the boundary of the particle-hole continuum. The wave-number q and frequency ω are normalized with respect to Fermi momentum k_F and Fermi energy ϵ_F , respectively. We set $a = 1$, $b = 15$, $m_1 = 1$, $m_2 = 1.25$, $k_F = 10$ and all $\epsilon = 1$ in the calculation.

both conduction and valence bands where the same dielectric constant $\epsilon_x^2 = \epsilon_1 \epsilon_2$ is found for all interactions. In the more general case $\epsilon_x^2 \neq \epsilon_1 \epsilon_2$, which arises quite naturally in the complex environment of EHL heterostructures, we can easily see from eq. (11) that the plasmon frequency scales as $\omega \sim \sqrt{q}$. There are two modes of plasmons.

For the OPS case with two screening layers, the interactions are respectively $V_{1,2} = \frac{2\pi e^2}{\epsilon_{1,2}q} (1 - e^{-qa}) \sim 2\pi e^2/\epsilon_{1,2} (a - a^2q/2)$ and $V_x = -\frac{2\pi e^2}{\epsilon_x q} e^{-qb} (1 - e^{-qa})^2 \sim -2\pi a^2 e^2 q/\epsilon_x$ for $q \ll a^{-1}$. Notice the removal of the $1/q$ singularity in the interactions by OPS. We then obtain after solving the equation the collective modes (up to order q^2)

$$\omega_{1,2} = \sqrt{\frac{2\pi a e^2 n_{1,2}}{m_{1,2} \epsilon_{1,2}}} \left(q - \frac{aq^2}{4} \right). \quad (12)$$

Notice that OPS effectively reduced the long-ranged Coulomb interaction into short-ranged interactions resulting in two collective modes scaling linearly with q . The collective modes represent separate collective motion of the two layers because $(V^x)^2$ is of higher order in q than $V_1 V_2$, and the inter-layer interaction appears only to order q^3 . For completeness, we have computed numerically the collective modes spectrums at finite q as shown in Fig. 2.

With only one screening layer, the interactions are $V_1(q) \sim \frac{2\pi e^2}{\epsilon_1} ((a + 2b) - (a + 2b)^2 q/2)$, $V_2(q) \sim \frac{2\pi e^2}{\epsilon_2} (a - a^2 q/2)$ and $V_x(q) = -\frac{2\pi e^2}{\epsilon_x q} e^{-qb} (1 - e^{-qa}) \sim$

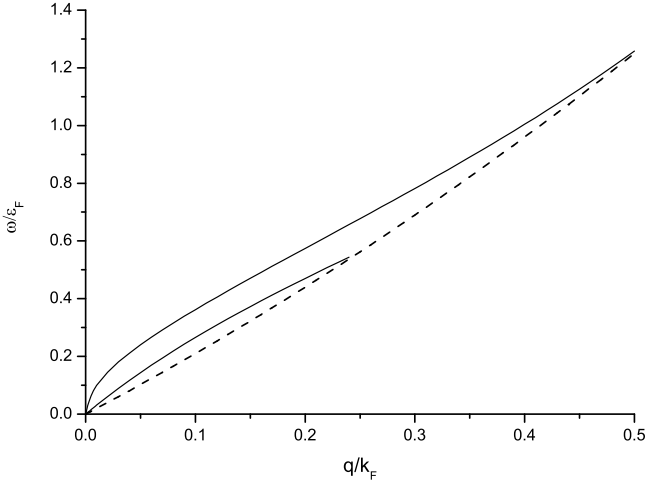


FIG. 3: Plasmon excitations in EHL with only one screening layer. At small q , both plasmon modes scale linearly with q with a larger slope $\propto \sqrt{2b+a}$ for ω_1 . We set $a = 1$, $b = 15$, $m_1 = 1$, $m_2 = 1.25$, $k_F = 10$ and all $\epsilon = 1$ in the calculation.

$-2\pi a e^2 / \epsilon_x$, respectively at small q . The collective modes are given by (up to order q^2)

$$\begin{aligned}\omega_1 &= \sqrt{\frac{2\pi(a+2b)e^2 n_1}{m_1 \epsilon_1}} \left(q - \frac{(a+2b)q^2}{4} \right) \\ \omega_2 &= \sqrt{\frac{2\pi a e^2 n_2}{m_2 \epsilon_2}} \left(q - \frac{a q^2}{4} \right).\end{aligned}\quad (13)$$

Again there are two linear plasmon modes and effect of V^x does not enter until q^3 . The main difference is that the electron-hole layer separation b enters the slope of ω_1 mode ($\propto \sqrt{2b+a}$). The numerically calculated plasmon spectrums are depicted in Fig. 3.

IV. EXCITON CONDENSATION AND WIGNER CRYSTALIZATION

In this section we study exciton condensation and Wigner crystalization in an electron-hole liquid with OPS. The system without OPS has been extensively studied for the search of exciton condensation. We shall consider exciton condensation in a BCS type mean-field theory where the exciton condensation is described by the order parameter $\langle c_{1k\uparrow} c_{2\bar{k}\downarrow} \rangle$ (1,2 are layer indices). For simplicity we assume the layers are doped with equal amount of charges (with opposite signs) and the electrons and holes are spin-polarized. Singlet pairing of excitons is implicitly assumed.

The EHL Hamiltonian in momentum representation

is

$$\begin{aligned}H &= \sum_{\alpha k} \xi_k^\alpha c_{\alpha k}^\dagger c_{\alpha k} + \sum_{pqk} V^x(k) c_{1p+k}^\dagger c_{2q-k}^\dagger c_{2q} c_{1p} \\ &+ \frac{1}{2} \sum_{\alpha p q k} V^\alpha(k) c_{\alpha p+k}^\dagger c_{\alpha q-k}^\dagger c_{\alpha q} c_{\alpha p},\end{aligned}\quad (14)$$

where $\alpha = 1, 2$ is the layer index; c_k (c_k^\dagger) is the momentum k fermion annihilation (creation) operator, $\xi_k^\alpha = \frac{k^2}{2m_\alpha} - \mu_\alpha$ is the electron or hole dispersion and $V^\alpha(k)$ ($V^x(k)$) is the intralayer (interlayer) OPS effective interaction. Next we employ the standard Hartree-Fock-Bogoliubov method [11] to derive the mean field equations for exciton condensate. The Hartree-Fock terms $\Sigma_k^\alpha = \sum_q V^\alpha(p-q) \langle c_{\alpha k}^\dagger c_{\alpha k} \rangle$ modify the particle dispersions $\xi_k^\alpha \rightarrow \xi_k^\alpha - \Sigma_k^\alpha$ and need to be solved self-consistently. Here we concentrate on the effect of exciton binding on the Fermi surface and shall assume that the self-energy can be captured by introducing effective masses m_α^* (ϵ_α) and renormalized chemical potentials μ_α^* (ϵ_α), i.e. $\xi_k^\alpha - \Sigma_k^\alpha \sim \frac{k^2}{2m_\alpha^*} - \mu_\alpha^*$. With this approximation, we obtain the mean field Bogoliubov Hamiltonian

$$H_{\text{MF}} = \sum_{k\sigma} \begin{pmatrix} c_{1k}^\dagger & c_{2\bar{k}} \end{pmatrix} \begin{pmatrix} \xi_k^1 & -\Delta_k \\ -\Delta_k & -\xi_k^2 \end{pmatrix} \begin{pmatrix} c_{1k} \\ c_{2\bar{k}}^\dagger \end{pmatrix}, \quad (15)$$

where

$$\Delta_k = - \sum_q V^x(k-q) \langle c_{1k} c_{2\bar{k}} \rangle \quad (16)$$

is the exciton order parameter. H_{MF} can be diagonalized easily by the Bogoliubov transformation

$$\begin{pmatrix} c_{1k} \\ c_{2\bar{k}}^\dagger \end{pmatrix} = \begin{pmatrix} u_k & v_k \\ -v_k & u_k \end{pmatrix} \begin{pmatrix} \gamma_{1k} \\ \gamma_{2\bar{k}}^\dagger \end{pmatrix}, \quad (17)$$

$$\begin{cases} u_k^2 = \frac{1}{2} \left(1 + \frac{\bar{\xi}_k}{E_k} \right), \\ v_k^2 = \frac{1}{2} \left(1 - \frac{\bar{\xi}_k}{E_k} \right), \end{cases} \quad (18)$$

where $E_k = \sqrt{(\bar{\xi}_k)^2 + \Delta_k^2}$, $\bar{\xi}_k = \frac{1}{2} (\xi_k^1 + \xi_k^2) \equiv \frac{k^2}{2m_{\text{eff}}} - \mu$, where $m_{\text{eff}}^{-1} = (m_1^{*-1} + m_2^{*-1})/2$ and $\mu = (\mu_1^* + \mu_2^*)/2$. The ground state wavefunction is

$$|\psi_G\rangle = \prod_k \left(u_k + v_k c_{1k}^\dagger c_{2\bar{k}}^\dagger \right) |0\rangle. \quad (19)$$

where Δ_k is determined by the self-consistent equation

$$\Delta_k = - \frac{1}{2} \sum_q V^x(k-q) \frac{\Delta_q}{E_q}. \quad (20)$$

The equation is to be solved with the particle number constraint

$$n = \sum_k v_k^2, \quad (21)$$

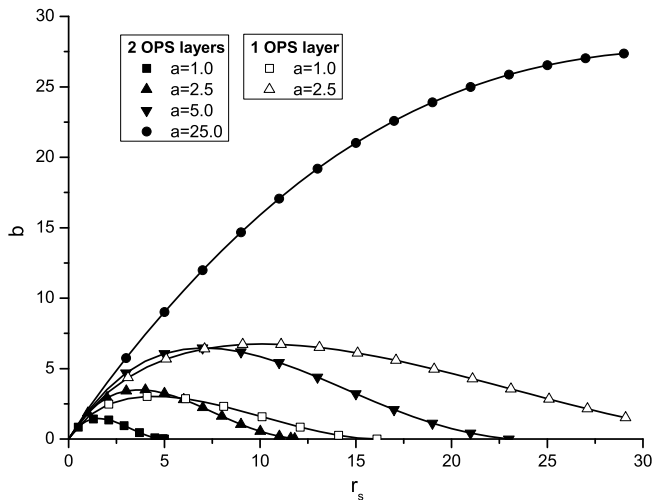


FIG. 4: The phase diagram for EHBL with two- and one-screening layers for varied image charge separation a . b is the bilayer separation and $r_s \sim \frac{1}{k_F}$ is the dimensionless average particle-particle separation in unit of the effective Bohr radius $a_B = \epsilon_x \hbar^2 / m_{\text{eff}} e^2$. Below the transition lines $b_c(r_s)$ an exciton gap Δ of magnitude larger than $10^{-5} \mu$ is formed.

where v_k^2 is the probability of finding an electron-hole pair in state k at the ground state. A zero-temperature phase diagram can be determined by numerically solving eqs. (20) and (21).

To simplify calculation we assume further that exciton gap is momentum independent $\Delta_k = \Delta$ and Δ is determined by minimizing the ground state energy. We note that we are considering a band structure with isotropic dispersion and the electron and hole Fermi surfaces are perfectly nested. In this case, the exciton pairing gap Δ is always non-zero in the mean-field theory, although its value can be very small. In reality the mean-field gap will be destroyed by quantum fluctuations when its magnitude is small [12], but this is not reflected in a mean field theory. To capture this physics qualitatively, we assume that the transition from the exciton condensed state to the normal state occurs at $\Delta = 10^{-5} \mu$. Although quantitatively unreliable, this procedure allows us to examine the effect of screening on the phase diagram semi-quantitatively as we shall see below.

With the above criteria, the phase diagram for different average particle-particle separation $r_s = \frac{1}{a_B} \sqrt{\frac{1}{\pi n}}$ (n is particle/hole density; $a_B = \epsilon_x \hbar^2 / m_{\text{eff}} e^2$ is the effective Bohr radius of electron-hole pair) and transition layer separation $b_c(r_s)$ can be determined by solving the self-consistent equations (20) and (21). We first consider EHBL with two screening layers. The result of calculation is depicted in Fig. 4 for different separation between the electron/hole and its image charge a (filled symbols).

In the small r_s (high density) regime, kinetic energy dominates over potential energy and the exciton pairing gap goes to zero as $r_s \rightarrow 0$. In large r_s or low density

limit, the exciton pairing is diminished due to the repulsive nature of the interlayer OPS potential at short distance (see Fig. 1(f)). This leads to a linear dependence of $V^x(k)$ versus k at small k (see eq. (3)). In this case, the gap equation eq. (20) is of the form $\int_0^{k_F} \frac{k}{\sqrt{\epsilon_k^2 + \Delta^2}} d^2 k = \text{constant}$ for small gap Δ , where $k_F \sim 1/r_s$ and larger r_s (smaller k_F) implies a smaller Δ to satisfy the equation. The electrons and holes need to be placed closer to each other to produce a large enough Δ and leads to the drop of $b_c(r_s)$ at large r_s . As the screening separation a increases, the transition line shifts upward as the interlayer OPS potential is strengthened which enhances pairing. For $a = 25$ (comparable with b), the image charge effect becomes negligible and potential becomes essentially Coulomb-like which permits exciton formation for all r_s we considered (cf. Fig. 1 in Ref. [12]). The main effect of OPS potential is to suppress exciton pairing at low density.

Previous numerical study of the same EHBL with no screening layer [12] reveals also an excitonic Wigner crystal phase at large r_s . Wigner crystal is commonly formed in low density (i.e. large r_s) electron liquid because of domination of Coulomb repulsive potential energy ($\sim 1/r_s$) over kinetic energy ($\sim 1/r_s^2$). To minimize the potential energy the electron wavefunction “crystalizes” to ensure maximum separation between electrons which yields the Wigner crystal phase. Here we argue that OPS suppresses the Wigner crystal phase in two ways. Firstly, as shown above, exciton formation is suppressed at large r_s and thus the *excitonic* Wigner crystal is unlikely to form. On the other hand, electronic Wigner crystals in separated layers are also prohibited since introduction of OPS reduces the (intralayer) potential energy and changes its scaling form to $\sim 1/r_s^3$ (dipolar interaction, see eq. (A.1)) at large particle separation $r \gg a$. In this case kinetic energy again dominates at large r_s and an usual electron/hole liquid phase should occur. The situation is similar to the case as found in Ref. [4] where the electronic Wigner crystal phase is destroyed by screening. We note, however that our simple study cannot rule out the possibility of having a Wigner crystal phase at some intermediate values of r_s where the kinetic and potential energies are of comparable magnitudes.

We now consider the situation of EHBL with only one screening layer which may be easier to realize experimentally (Fig. 1(c)). In this case we adopt eq. (5) for interlayer interaction, where $V^x(k)$ scales as constant at small k . We can again consider the gap equation and argue similarly that the exciton phase boundary would also drop at large r_s , as in the two-layer screening case. Indeed we have solved the gap equations and find that the phase diagram is qualitatively the same as the two OPS layer case except that the area under the phase boundary $b_c(r_s)$ is larger (see Fig. 4 (open symbols)).

For the Wigner crystal phase, the “asymmetric” OPS introduces some complications. First we note that an

excitonic Wigner crystal phase is also unlikely to occur at large r_s . However the system may form a hybrid phase where a Wigner crystal is formed at layer 1 and electron/hole liquid phase remains for layer 2 because screening mainly affects layer 2. To examine this possibility we check the effective intralayer interaction after taking into account the screening effect of the other charged layer (see eq. (A.1) in Appendix and discussions thereafter). We see that the effective intralayer interaction is mainly dominated by $V_{1,2}^{\text{intra}}(q)$, and screening from the other layer is not important. Therefore, we expect that at large r_s kinetic energy again dominates and the both layers are in the electron/hole liquid phase. Notice, however that $V_1^{\text{intra}}(q)$ has a dipolar form only when $r_s \sim r/a_B \gg b/a_B$ for layer 1. Thus for some large enough b/a_B , a hybrid phase (Wigner crystal at layer 1, electron/hole liquid at layer 2) may still occur at some intermediate densities $b/a_B \gg r_s \gg 1$.

We see that OPS becomes important for low density electronic systems due to change in scaling of the potential energy. Generally speaking, for heterostructures, insulating behavior resulting from low carrier density can be avoided by addition of metallic screening layers [4]. This method may be preferred over other methods like increasing carrier density by dopants since dopants act like impurities and introduce unnecessary scattering at low temperature.

V. STRONGLY CORRELATED EHBL

In strongly correlated materials, the basic electronic properties are determined by the bandwidth, the on-site Coulomb interactions U and the charge transfer energy E_c . If such a ultra-thin film, originally a Mott insulator, is placed close to a metal surface, U and E_c can be strongly reduced by OPS [7]. When the bandwidth exceeds the suppressed U and E_c , the insulating film can undergo an insulator-metal phase transition. Furthermore, if a heterostructure is formed, structural relaxation and local electronic states may exist at the interfaces. For instance, in an interface formed by $\text{YBa}_2\text{Cu}_3\text{O}_7$ (YBCO) cuprate and metal [8, 9], the CuO_2 plane near the interface (depletion layer) is intrinsically doped by electronic reconstruction resulting in a strongly correlated electron system with OPS interaction induced by the metal. We shall consider here how OPS would affect the properties of this system.

The mean field analysis on effect of OPS can also be performed for strongly correlated EHBL systems [13, 14] with a two-layer t - J type model. We assume here that the suppression of U and E_c induced by OPS are not strong enough to destroy strong correlation, otherwise we can simply apply the usual electron-hole liquid picture described in previous section. Therefore the setting is similar to that shown in Fig.1(b) except that the electron-hole liquid is replaced by a strongly correlated EHBL with holons and doublons and the excitons

are formed by holon-doublon pairs instead of electron-hole pairs. A mean field calculation similar to that of Ref.[13] can be carried out by applying the slave-boson mean field theory to the two-layer t - J model. The main difference is that the on-site interlayer interaction $V_0 \sum_i b_{1i}^\dagger b_{1i} b_{2i}^\dagger b_{2i}$ is replaced by the OPS effective interaction $\sum_{ij} V_{ij}^x b_{1i}^\dagger b_{1i} b_{2j}^\dagger b_{2j}$, where $b_{\alpha i}$ ($b_{\alpha i}^\dagger$) is the bosonic holon ($\alpha = 1$) or doublon ($\alpha = 2$) annihilation (creation) operator of layer α at site i . The OPS interaction is then decoupled as

$$\begin{aligned} \sum_{ij} V_{ij}^x b_{1i}^\dagger b_{1i} b_{2j}^\dagger b_{2j} &\xrightarrow{\mathcal{F}} \sum_{pqk} V_k^x b_{1p}^\dagger b_{2q}^\dagger b_{2q+k} b_{1p-k} \\ &\approx \sum_p \Delta_p^b \left(b_{1p} b_{2\bar{p}} + b_{2\bar{p}}^\dagger b_{1p}^\dagger \right) \\ &\quad - \sum_p \Delta_p^b \langle b_{1p} b_{2\bar{p}} \rangle, \end{aligned}$$

where $\Delta_p^b = \sum_q V_{p-q}^x \langle b_{1q} b_{2\bar{q}} \rangle$ is the exciton pairing. Assuming that $\Delta_p^b = \Delta^b \delta(p)$ is homogeneous in space, we obtain a mean field Hamiltonian which is of the same form as in previous study [13] for on-site interaction V_0 with $\langle b_{1i} b_{2i} \rangle \sim \sum_k \langle b_{1k} b_{2\bar{k}} \rangle$. Since in terms of exciton pairing the attract-repel behavior renders the interlayer OPS interaction resembling an on-site interaction (see Fig.1(f)), we expect that the mean field phase diagrams in both case are qualitatively the same. The introduction of OPS interaction solely shifts the exciton phase boundary due to a reduction of interaction strength, as in the case of usual electron-hole liquid.

We next comment on the possibility of forming spatially inhomogeneous phases. One example of such inhomogeneity is charge corrugation in the form of stripes. By applying mean field theory to t - J model with long range Coulomb interaction $V_c \sum_{i \neq j} \frac{1}{r_{ij}} n_i n_j$, it is shown that stripes are preferred to minimize the exchange J term [15]. In particular, it is the decoupling of the exchange term into the anti-ferromagnetic channel m_i that drives the stripe formation, while the Coulomb interaction controls the spacing evolution of stripes with doping. Moreover, the stripes spacing increases as the doping δ decreases. The effect of OPS on stripes is two-fold. Firstly, OPS weakens the on-site repulsion U [16] and thus the superexchange $J \sim t^2/U$ term is enhanced (assuming that strong correlation is still intact). Consequently, the stripes phase is strengthened. On the other hand, Coulomb interaction tends to smooth out the charge density, while a dipolar interaction ($V \sim 1/r^3$ for large r) would be less effective and a more inhomogeneous phase would be preferred. Notice that extreme charge inhomogeneity like phase separation [17] is not likely since the OPS interaction scales like $1/r$ for small r and still suppresses phase separation.

VI. SUMMARY

We have constructed a dipolar interaction for OPS effect of metallic layer in heterostructures and have justified the construction by a RPA calculation. The OPS interaction is expected to be present rather generally at interfaces with metallic layers. We apply the OPS interaction to EHBL system and find that OPS mainly affects the electronic properties in the low density regime. Our conclusion is not restricted to EHBL since the behavior is mainly due to the modification of the interaction scaling from $1/r$ (Coulomb) to $1/r^3$ (dipole) at distance of large r . OPS might be employed to eliminate Wigner-crystal like behavior at low temperatures. For strongly correlated electron systems, OPS mainly affects the magnetic channel by reducing the Hubbard U and charge transfer energy E_c . The reduction of U may drive the system into usual electron liquid. Furthermore, the reduction in interaction range may drive the system into an inhomogeneous state.

Acknowledgments

We acknowledge Prof. P. A. Lee and Prof. N. Nagaosa for insightful comments and Dr. Y. Zhou, Dr. X. Y. Feng, C. K. Chan and Z. X. Liu for helpful discussions.

Appendix: Justification of OPS interactions by RPA

In this appendix, we employ RPA to justify the image-charge picture of OPS interactions. The RPA method enables us to obtain an effective interaction by “integrating out” the screening layers.

First we consider a charged layer 2 with a metallic screening layer s separated from layer 2 by distance $a/2$, as shown in Fig. 1(c). We can write down the effective intralayer interaction of layer 2 after taking into account the effect of screening by the metallic layer (see Fig. 5)

$$\begin{aligned} V^{\text{intra}}(q) &= V_2(q) + \frac{V_{2s}(q)\chi_{0s}V_{s2}(q)}{1 - \chi_{0s}V_{ss}(q)} \\ &= 2\pi e^2 \left(\frac{1}{q} - \frac{e^{-aq}}{q} \frac{2\pi e^2 N_F}{q + 2\pi e^2 N_F} \right) \\ &\approx \frac{2\pi e^2}{q} (1 - e^{-aq}) , \end{aligned}$$

where $V_2(q) = V_{ss}(q) = 2\pi e^2/q$ are the bare Coulomb interactions of layer 2 and screening layer s , $V_{2s}(q) = V_{s2}(q) = 2\pi e^2 e^{-aq/2}/q$ is the interlayer Coulomb interaction between the layers, and $\chi_{0s} = \chi_{0s}(q \rightarrow 0, \omega = 0) = -N_F$ is the $q \rightarrow 0$ static density-density response function [10] of layer s , N_F is density of states at the Fermi surface. Notice we have assumed that q is small (long wavelength limit) in writing down the interactions and

$$2 \text{---} 2 = 2 \text{---} 2 + 2 \text{---} \text{bubble} \text{---} 2 + 2 \text{---} \text{bubble} \text{---} \text{bubble} \text{---} 2 + \dots$$

FIG. 5: Diagram for construction of OPS interactions. Thin lines are bare interactions, bubble is the density-density response function χ_{0s} and the thick line is the resulting effective interaction.

therefore

$$F_0 \equiv \frac{2\pi e^2 N_F}{q + 2\pi e^2 N_F} \approx 1 .$$

This approximation is valid if the charge density n_2 of layer 2 is much less than the density of the screening layer n_s and $q \lesssim \sqrt{n_2} \ll \sqrt{n_s}$. We shall take the same limit in the following derivations. This gives eq. (2).

Similarly we can construct the interlayer interaction eq. (5):

$$\begin{aligned} V^{x,1}(q) &= V_{12}(q) + \frac{V_{1s}(q)\chi_{0s}V_{s2}(q)}{1 - \chi_{0s}V_{ss}(q)} \\ &= 2\pi e^2 \left(\frac{e^{-bq}}{q} - \frac{e^{-(a+b)q}}{q} F_0 \right) \\ &\approx 2\pi e^2 \frac{e^{-bq}}{q} (1 - e^{-aq}) , \end{aligned}$$

where $V_{12}(q) = 2\pi e^2 e^{-bq}/q$, $V_{1s}(q) = 2\pi e^2 e^{-(a/2+b)q}/q$ and $V_{s2}(q) = 2\pi e^2 e^{-aq/2}/q$ are the bare interlayer interactions between the pair of layers (1,2), (1, s) and (s , 2) respectively. For two screening layers (Fig. 1(b)), we assume that layer 2 and s form an effective system 2' and thus we can adopt $V^{x,1}$ as the “bare” interlayer interactions in the following:

$$\begin{aligned} V^{x,2}(q) &= V^{x,1}(q) + \frac{V_{1s}(q)\chi_{0s}V_{s2'}(q)}{1 - \chi_{0s}V_{ss}(q)} \\ &= 2\pi e^2 (1 - e^{-aq}) \left(\frac{e^{-bq}}{q} - \frac{e^{-(a+b)q}}{q} F_0 \right) \\ &\approx 2\pi e^2 \frac{e^{-bq}}{q} (1 - e^{-aq})^2 , \end{aligned}$$

where $V_{s2'}(q) = V^{x,1}(b \rightarrow b + \frac{a}{2}) = \frac{1}{q} e^{-(\frac{a}{2}+b)q} (1 - e^{-aq})$. The validity of assuming the effective system 2' is based on the choice of $b \gg a$. This gives eq. (3).

Here we derive the effective intralayer interaction $V_{1,\text{eff}}^{\text{intra}}(q)$ with two-layer OPS (Fig. 1(b)) taking into account the screening of system 2' (i.e. integrated out all the screening by 2, $s1$ and $s2$):

$$V_{1,\text{eff}}^{\text{intra}}(q) = V_1^{\text{intra}}(q) + \frac{\chi_{02} (V^{x,2}(q))^2}{1 - V_2^{\text{intra}}(q)\chi_{02}} . \quad (\text{A.1})$$

In the small q limit, $V^{x,2}$ and V_2^{intra} scale as q and constant respectively. The second term due to screening is of higher order in q and thus it cannot alter the scaling of the $V_1^{\text{intra}}(q)$ term (\sim constant). One can repeat the

analysis for the one-layer OPS case (see Fig. 1(c)) and the scaling of the effective intralayer interaction $V_{1,2}^{\text{intra}}(q)$ in the lowest order of q is not affected by screening of the opposite charged layer.

-
- [1] S. Okamoto and A. J. Millis, *Nature* **428**, 630 (2004).
 [2] X. Hong, T. Ishihara and A. V. Nurmikko, *Phys. Rev. B* **45**, 6961 (1992).
 [3] E. A. Mulijarov, S. G. Tikhodeev and N. A. Gippius, *Phys. Rev. B* **51**, 14370 (1995).
 [4] J. Huang, D. S. Novikov, D. C. Tsui, L. N. Pfeiffer and K. W. West, *Phys. Rev. B* **74**, 201302(R) (2006). See also, L. H. Ho *et al.*, *Phys. Rev. B* **77**, 201402(R) (2008).
 [5] L. H. Ho, A. P. Micolich, A. R. Hamilton and O. P. Sushkov, *Phys. Rev. B* **80**, 155412 (2009).
 [6] Sen Yang, A. T. Hammack, M. M. Fogler and L. V. Butov, *Phys. Rev. Lett.* **97**, 187402 (2006).
 [7] S. Altieri, L. H. Tjeng and G. A. Sawatzky, *Thin Solid Films* **400**, 9-15 (2001).
 [8] U. Schwingenschlögl and C. Schuster, *Europhys. Lett.* **77**, 37007 (2007).
 [9] U. Schwingenschlögl and C. Schuster, *Phys. Rev. B* **79**, 092505 (2009).
 [10] See, e.g., G. F. Giuliani and G. Vignale, *Quantum Theory of the Electron Liquid* (Cambridge University Press, Cambridge, 2005).
 [11] See, e.g., Xuejun Zhu, P. B. Littlewood, Mark S. Hybertsen and T. M. Rice, *Phys. Rev. Lett.* **74**, 1633 (1995).
 [12] S. De Palo, F. Rapisarda and Gaetano Senatore, *Phys. Rev. Lett.* **88**, 206401 (2002).
 [13] Jung Hoon Han and Chenglong Jia, *Phys. Rev. B* **74**, 075105 (2006).
 [14] T. C. Ribeiro, A. Seidel, J. H. Han and D.-H. Lee, *Europhys. Lett.* **76**, 891 (2006).
 [15] Junghoon Han, Qiang-Hua Wang and Dung-Hai Lee, *Int. J. of Mod. Phys. B* **15**, 1117 (2001).
 [16] S. Altieri *et al.*, *Phys. Rev. B* **79**, 174431 (2009).
 [17] V. J. Emery, S. A. Kivelson and H. Q. Lin, *Phys. Rev. Lett.* **64**, 475 (1990).